

Engine Contribution Analysis Using a Noise and Vibration Simulator

Andreas Schuhmacher and Dimitri Tcherniak, Brüel & Kjær, Nærum, Denmark

We investigated a pure time-domain version of source-path-contribution analysis using a controllable source, a noise and vibration simulator installed into a trimmed vehicle. We examined both airborne and structure-borne inputs, and used the matrix method in the time-domain to calculate source contributions as sounds at a listeners' position inside the cabin. Operating data from a simulated run-up/run-down and sets of transfer functions (FRFs) are used first to estimate the strength of some defined point sources, both acoustically and mechanically. Second, the operating source strengths are combined with acoustic or vibro-acoustic FRFs to predict contributions at a receiver. Here we attempted to make the airborne and structure-borne models as simple as possible, and predicted contributions are validated against actual measured data. All measurements were conducted on the vehicle with and without the engine simulator installed.

Airborne and structure-borne source-path-contribution analysis plays an important role in the automotive industry as a tool to identify and quantify contributions from sources to receiver locations inside a cabin. Depending on the nature of the excitation, contributions can be split into airborne or structure-borne, and several techniques for estimating individual contributions exist. In case of structure-borne inputs, a set of unknown input strengths, or input point forces, can be estimated using indirect techniques, since the acting force on the vehicle body under operation cannot be measured directly in a reliable way.

There are two conventional indirect techniques:

- Mount stiffness based on stiffness data estimates of rubber mounts.
- Matrix method that uses vibration transfer functions (accelerances) for the trimmed vehicle.

In theory the second measurement requires that the engine be removed from the rest of the vehicle, complicating the measurement procedure. Having estimated the forces during operation, vibro-acoustic transfer functions (noise transfer functions) relating to sound pressure at a receiver to the input force can be used to do the contribution analysis; i.e., finding the dominant contribution, strongest path, etc.

For the airborne approach the matrix method is usually used, where acoustic transfer functions and operating data are combined to form an acoustical model of the engine. A new set of acoustic transfer functions makes it possible to investigate contributions to a desired receiver. When doing the measurements for the acoustical source modelling, the engine is normally removed and placed on an engine test bench, but here we consider the engine installed during all measurements.

A noise and vibration engine simulator is used to produce airborne and structure-borne inputs to a vehicle body through some simple mounts and via the built-in loudspeakers. The inputs can be controlled to produce either airborne and/or structure-borne inputs. The predicted total contribution inside the cabin from the engine simulator is validated against the actual measured data. The different numerical issues associated with matrix inversion are discussed, and attention is also paid to some practical measurement aspects.

Matrix Inversion Method

The method considered in this study is a version of the matrix method, in the time domain. It applies to both the structure-borne and the airborne cases. In either case, the sources are modelled

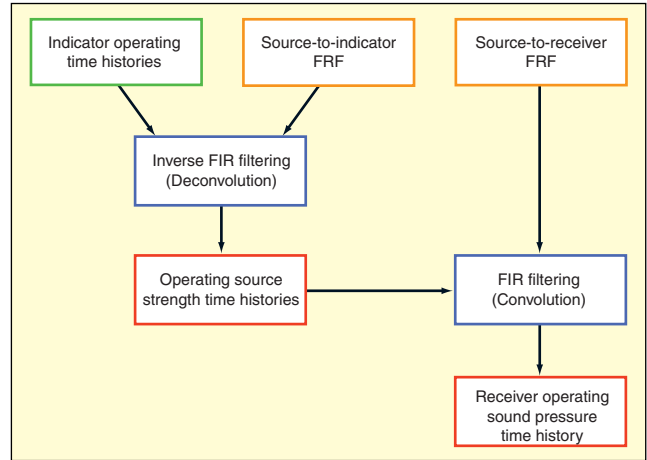


Figure 1. Time-domain process to obtain receiver contributions from indicator time histories and FRFs.

by a number of point sources – acoustical point sources in the airborne case or point forces including a certain direction in the structure-borne case.^{1,2} Rotational degrees of freedom are neglected throughout this work. Usually an indirect procedure is used to estimate the strength of each point source in the model. This involves measuring operating data at so-called indicator positions close to the selected point source positions and also to determine transfer functions between each point source position and all indicator positions. Finally, matrix inversion techniques can be used to estimate the source strengths for the two cases.

Frequency Domain. The usual approach is to write the matrix method in the frequency domain, solving a matrix equation for each frequency line. For the two cases, it can be written:

$$\mathbf{q} = \mathbf{H}_{AB}^{-1} \mathbf{p}_{ind}, \quad \mathbf{f} = \mathbf{H}_{SB}^{-1} \mathbf{a}_{ind} \quad (1)$$

Here \mathbf{q} is a vector of acoustical source strengths matching the operating data at indicator microphones in \mathbf{p}_{ind} . For structure-borne, \mathbf{f} contains operating forces obtained from operating vibration data at indicator accelerometers in \mathbf{a} . Transfer functions are measured as frequency response functions (FRFs) and arranged in the two matrices. For airborne contributions, a source with known volume velocity output is put to each defined source position, and the sound pressure is measured at the indicator microphones. The obtained pressure/volume velocity FRFs are arranged in the matrix \mathbf{H}_{AB} . Similarly for structure-borne contributions, a known force is applied at the defined force input points, and acceleration is measured at indicator accelerometers. The measured accelerances, acceleration/force, are arranged in the matrix \mathbf{H}_{SB} .

In both cases, care should be taken when inverting the matrix, since it can become ill-conditioned; however, regularization methods to overcome this problem and enabling calculation of a useful solution to the matrix problem exist.³

Having calculated the point source strengths under operation, the next step is to do the actual contribution analysis by simply multiplying source strength with a transfer function to the receiver. If we only consider an acoustical receiver, the sound pressure is:

$$P_{rec} = \sum_i H_{rec,i} q_i, \quad P_{rec} = \sum_j H_{rec,j} f_j \quad (2)$$

where H_{rec} are acoustic (pressure/volume velocity) or vibro-acoustic (pressure/force) transfer functions. These calculations make it possible to investigate how much a certain physical source, represented by a point source in the model, contributes to the total

Based on a paper presented at ISMA2006, the 2006 conference on Noise and Vibration Engineering, Leuven, Belgium, September 2006.

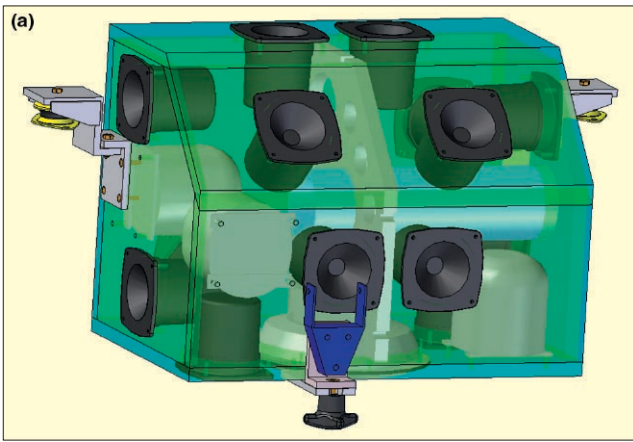


Figure 2. Engine noise and vibration simulator placed in vehicle.

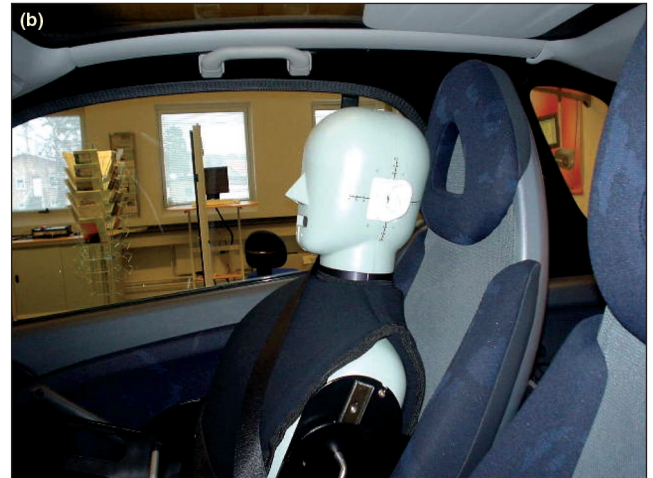


Figure 3. Trimmed vehicle for acceleration and vibro-acoustic FRF measurements.

sound pressure level at a receiver location.

Since amplitude and phase is measured for all FRFs, a fully coherent operating dataset must be supplied when solving the matrix equation, otherwise principal component decomposition should be used in a preprocessing step.

Time Domain. Instead of relying on the frequency-domain method, a time-domain method would make it possible to easily handle nonstationary conditions like an engine run-up/run-down. Furthermore, the contribution results are in the form of time signals (sounds), allowing all sorts of postprocessing to be done later.

A time-domain version of the above equations can be established if we consider a matrix of inverse time filters to be used in a deconvolution process. For the two cases:

$$\text{Airborne: } \begin{bmatrix} q_1(t) \\ \vdots \\ q_n(t) \end{bmatrix} = \begin{bmatrix} \text{Airborne} \\ \text{Inverse Filter Matrix} \end{bmatrix} * \begin{bmatrix} p_{ind,1}(t) \\ \vdots \\ p_{ind,m}(t) \end{bmatrix} \quad (3)$$

$$\text{Structure-borne: } \begin{bmatrix} f_1(t) \\ \vdots \\ f_n(t) \end{bmatrix} = \begin{bmatrix} \text{Structure-borne} \\ \text{Inverse Filter Matrix} \end{bmatrix} * \begin{bmatrix} a_{ind,1}(t) \\ \vdots \\ a_{ind,m}(t) \end{bmatrix} \quad (4)$$

where '*' is the convolution operator.

The inverse filter matrices are obtained from matrix inversion for all relevant frequencies and then turned into FIR filters. As a result, the point source strengths will now be in the form of time histories.

Receiver contributions are calculated by convolution with another set of FIR filters h representing the path between source and receiver:

$$p_{rec}(t) = \sum_i h_{rec,i} * q_i(t) \quad , \quad p_{rec}(t) = \sum_i h_{rec,j} * f_j(t) \quad (5)$$

The complete process of getting receiver operating sound pressure time data from operating data at indicator transducers is shown in Figure 1.

Engine Noise and Vibration Simulator Measurements

A noise and vibration simulator made as a wooden box with seven faces was used as source for testing the time-domain contribution analysis method. Each face is equipped with several loudspeaker units for producing pure airborne inputs into the vehicle body under consideration. Also, a ButtKicker shaker installed inside the wooden box is used to generate pure structure-borne inputs. This way, we can control the source to produce only airborne inputs or structure-borne inputs or combinations of both. For the airborne case, individual signals can be fed to the faces, which can be turned on and off, making it possible to validate the face contributions. The simulator box is installed into a Smart Car through three mounts (see Figure 2).

Operating Measurements. Engine bay recordings made during operating tests on a different vehicle were played through the engine faces, and a further set of signals was used as input to the shaker inside the simulator box. The signals considered in this work were all taken from a run-up/run-down.

For the structure-borne matrix method, acceleration signals measured on the vehicle body side are needed to calculate operating forces at selected positions and for selected directions. One tri-axial accelerometer (B&K 4520) was fastened to the vehicle body close to each mounting point. An extra four uni-axial accelerometers (B&K 4507 Bx) distributed on the frame were used to provide more information for the force estimations and create a slightly overdetermined system of equations. This gives a total of 13 accelerometer signals.

For the airborne matrix method, we decided to model the simulator using seven acoustical point sources, one representing each face. Seven indicator microphones (B&K 4935) were placed on the engine bay walls around the simulator, one microphone in front of each face.

The two microphones of a head and torso simulator (HATS)

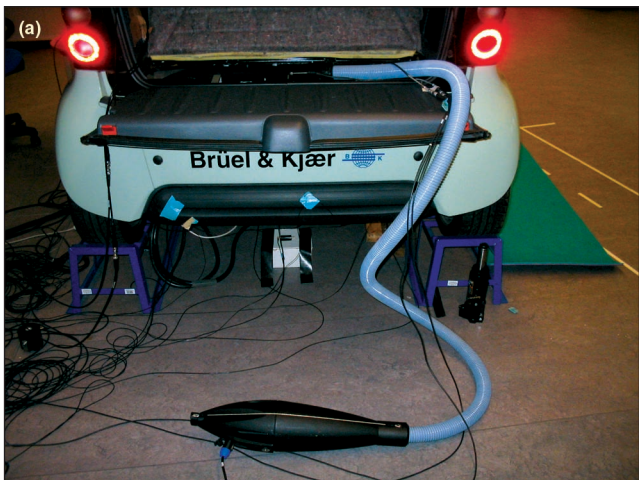


Figure 4. Volume velocity source used for acoustic FRF measurements.

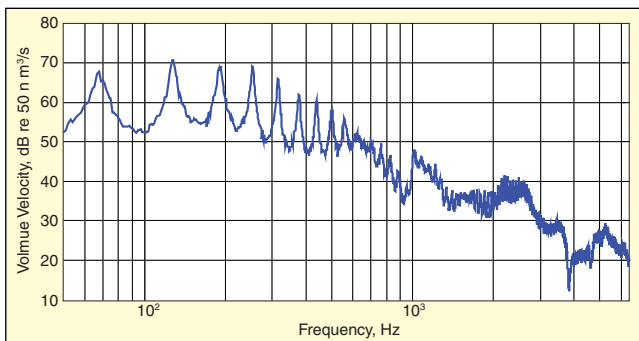


Figure 5. Volume velocity output spectrum for sound source incl. hose.

positioned on the passengers seat take the role as acoustical receivers (see Figure 3).

Simultaneous recordings of time histories for all the above signals were made for different scenarios: airborne and structure-borne excitation, airborne only, structure-borne only, and finally, exciting each face (airborne). A sampling rate of 16,384 Hz was used for all recordings, resulting in a bandwidth of 6.4 kHz.

FRF Measurements. The matrix method for structure-borne analysis needs an accelerance matrix to be used in an inverse problem for estimating a set of operating forces acting on the vehicle body. Prior to mounting the engine simulator inside the engine bay of the Smart Car, this matrix was measured using the same set of accelerometers as for the operating tests. The structure-borne excitation of the vehicle body caused by the engine simulator was considered modelled as three forces in the x, y, and z-direction acting on the vehicle body at each mount, for nine forces in total. A hand-held mini shaker provided the input force, and FRFs to all accelerometers were measured. This was done for the three mounting points in three directions, resulting in a $13 \times$

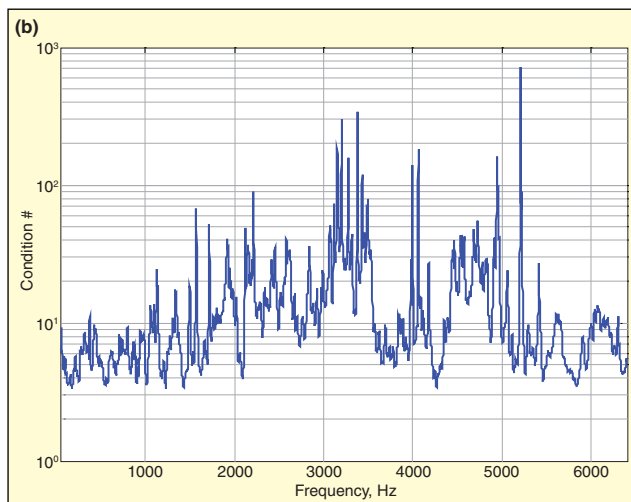
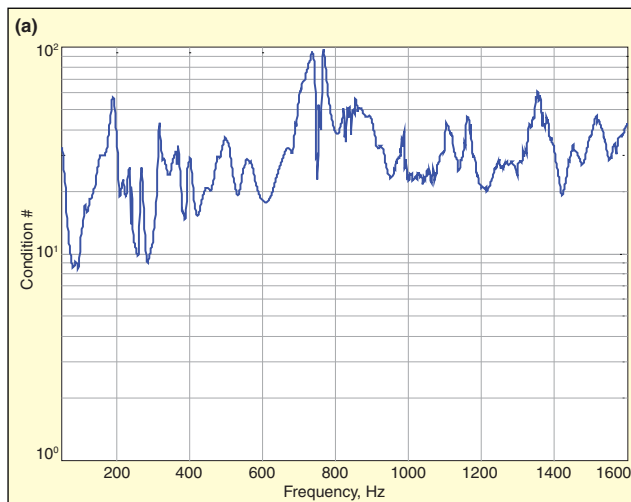


Figure 6. Condition number vs. frequency for structure-borne matrix (a) and airborne matrix (b).

9 accelerance FRF matrix for the structure-borne matrix inversion problem. The FRFs were measured up to 1.6 kHz with a frequency resolution of 1 Hz.

The trimmed vehicle without engine simulator mounted is shown in Figure 3. At the same time of measuring the accelerance FRFs, vibro-acoustic transfer functions (also called noise transfer functions) from the force input positions and directions were measured to the two HATS receiver microphones inside the vehicle. This would give a more consistent dataset of FRFs; however, an alternative to measuring the vibro-acoustic transfer functions in the direct sense would be to measure reciprocally with acoustical excitation at the HATS ears measuring acceleration at the mounts.

We decided to make an acoustical model of the engine simulator with a small number of acoustical point sources, only one source placed on each engine face in the center, for a total of seven acoustical sources. For estimating the operating source strength of each source, one indicator microphone was positioned in front of each face. The acoustic FRF matrix is measured using a calibrated volume velocity source (B&K 4295 OmniSource™ fitted with a flexible hose and volume velocity adaptor), as shown in Figure 4. The volume velocity output at the opening of the adaptor is measured using a pair of phase-matched microphones; this is then used to determine the volume velocity-to-sound pressure transfer functions needed for this study. All acoustic transfer functions were measured up to 6.4 kHz with a frequency resolution of 1 Hz with this single-volume velocity source. In the low frequency end, the output from this source begins to become poor below 50 Hz, so the transfer functions will be less valid in that region.

Figure 5 shows an example of the volume velocity output spectrum during measurement and the effect of the hose producing some peaks in the spectrum is observed. The nozzle of the volume

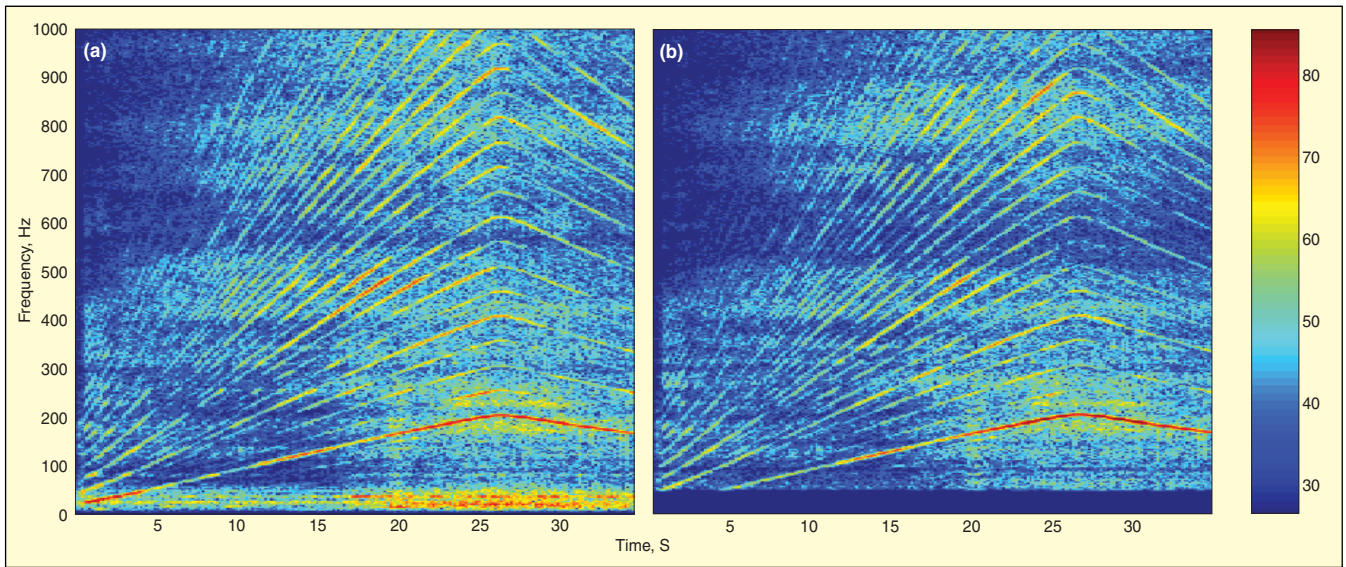


Figure 7. Spectrograms (frequency vs. time) of total (airborne and structure-borne) measured sound (a) and predicted sound (b) at left ear position.

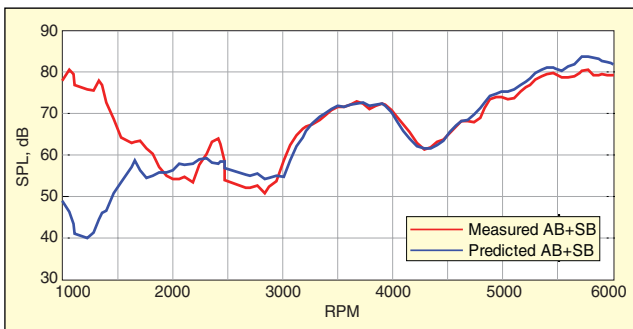


Figure 8. 2nd order contributions – total (airborne and structure-borne) measured vs. predicted.

velocity source was fastened to each engine face, and acoustic FRFs were measured to all indicator microphones and the two HATS microphones. This provided a 7×7 acoustic FRF matrix for the inverse determination of acoustical source strengths.

Analysis and Contribution Results

Data Processing. The first step in the time-domain approach is to convert the measured FRFs into inverse filters for the deconvolution step. Having assembled the two matrices for our analysis, an inversion step is necessary for each frequency. To do that properly, a picture of the matrix ill-conditioning is useful. The matrix condition number is a measure of how sensitive the solution is to errors in the data or the matrix itself. Figure 6 shows two plots of condition number versus frequency for the two matrices. In both cases, the condition number is within the range of 10-100 for most frequencies, meaning that it is not severely ill-conditioned.

On the other hand, to avoid solutions containing amplified noise components, a singular value decomposition (SVD) is carried out for each frequency line, and singular values smaller than a certain threshold are discarded. In this work, this threshold is expressed in dB relative to the largest singular value, and a 20-dB value has been applied in both cases. A threshold of 20 dB means that the resulting matrix condition number will be 10 for all frequencies. For the airborne matrix below 1000 Hz, Figure 6b shows that the chosen threshold will have no effect, since the condition number is already below 10. Below 50 Hz, the measured FRFs are not expected to be valid, so this very low frequency range is filtered out before creating the inverse FIR filters. For the contribution calculations, a second set of FIR filters is created, representing the paths between point sources and in-cabin receivers.

The operating data for the contribution calculations will be the time histories recorded at indicator microphones and indicator accelerometers when all airborne and structure-borne inputs of the engine simulator are active, as would be the case for an actual

operating engine. The 13 indicator accelerometer time histories are filtered through the structure-borne inverse filters to get the nine operating forces as time signals, which can be further filtered to get sound pressure time signals at either left or right HATS receiver position. For the airborne contributions, the seven indicator microphone time histories are filtered through the airborne inverse filter matrix to determine the seven operating volume velocity source strengths, which can also be further filtered to get receiver contributions.

Contribution Results. If we sum the contributions from the nine operating forces and the seven operating volume velocity sources, we get a modelled prediction of the total structure-borne and airborne engine sound inside the cabin at the HATS left and right ear position. To validate the model of the engine simulator, a comparison is made with the total measured sound. Spectrograms showing frequency contents vs. time of the total predicted sound and the total measured sound at the left ear are shown in Figure 7. Only frequencies up to 1 kHz are shown. The two plots show similar features, and the missing frequencies below 50 Hz are noticeable for the prediction. From the original engine recordings made inside the real vehicle, the second engine order is the most dominant feature. Those original recordings are input to the engine simulator explaining why the plots also show a dominating second order.

An Autotracker based on a statistical framework⁴ eliminates the need for a corresponding tacho signal and was therefore used to estimate RPM as a function of time from the left-ear acoustical time signals. Having estimated an RPM profile, the second-order contributions for the run-up section of the signals can be plotted together (see Figure 8). Except for the very low RPMs, which are affected by the 50-Hz high-pass filtering in the predictions, the measured and predicted levels for this order agree very well.

Since we have measured operating data for the structure-borne and airborne inputs alone, we can make a further validation into these components. Comparisons of left-ear spectrograms for structure-borne-only excitations are shown in Figure 9. For this type of input, the left-ear signals are really dominated by the second-order component. Some higher orders are noticeable in the spectrogram of the measured signal but are not significant in the predicted result. The corresponding second-order contributions are plotted in Figure 11, where the effect of regularization in the inverse filter calculations, which then further affects the predictions, is introduced.

So far, we have assumed some kind of regularization when calculating the inverse filters for the predictions in either case (blue curve). If we do not add any regularization in the inverse filter calculations, meaning that we just compute the pseudo-inverse of the matrices for each frequency, we get another set of inverse filters. Using this other set of filters in the structure-borne case, we

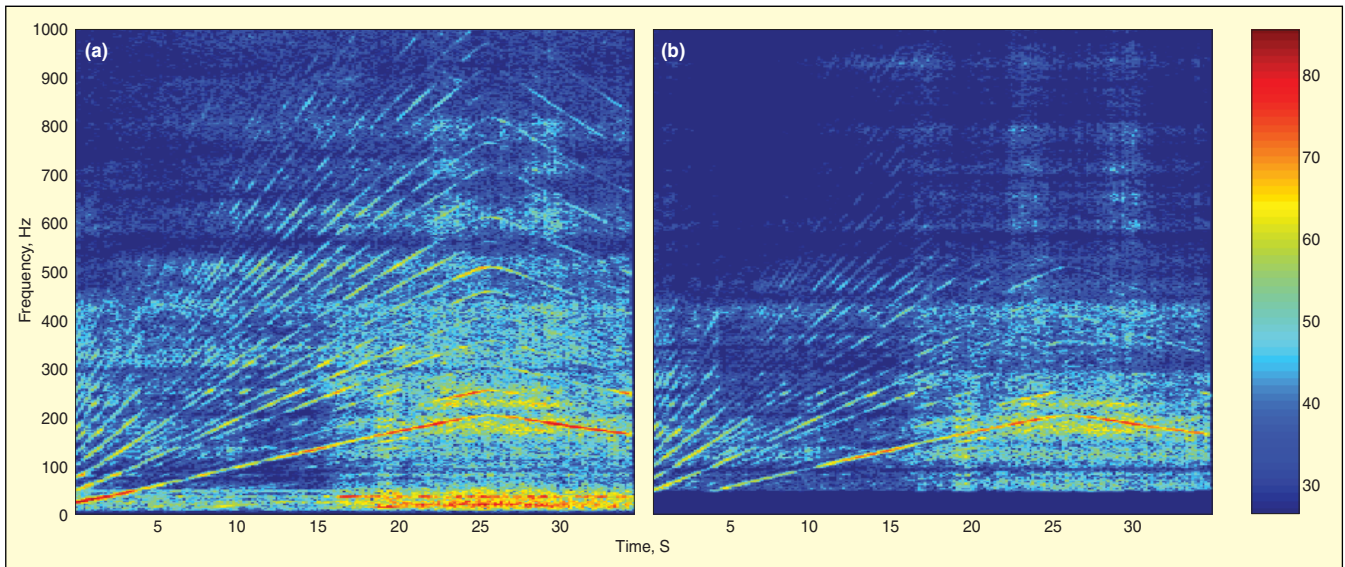


Figure 9. Spectrograms (frequency vs. time) of structure-borne measured sound (a) and predicted sound (b) at left ear position.

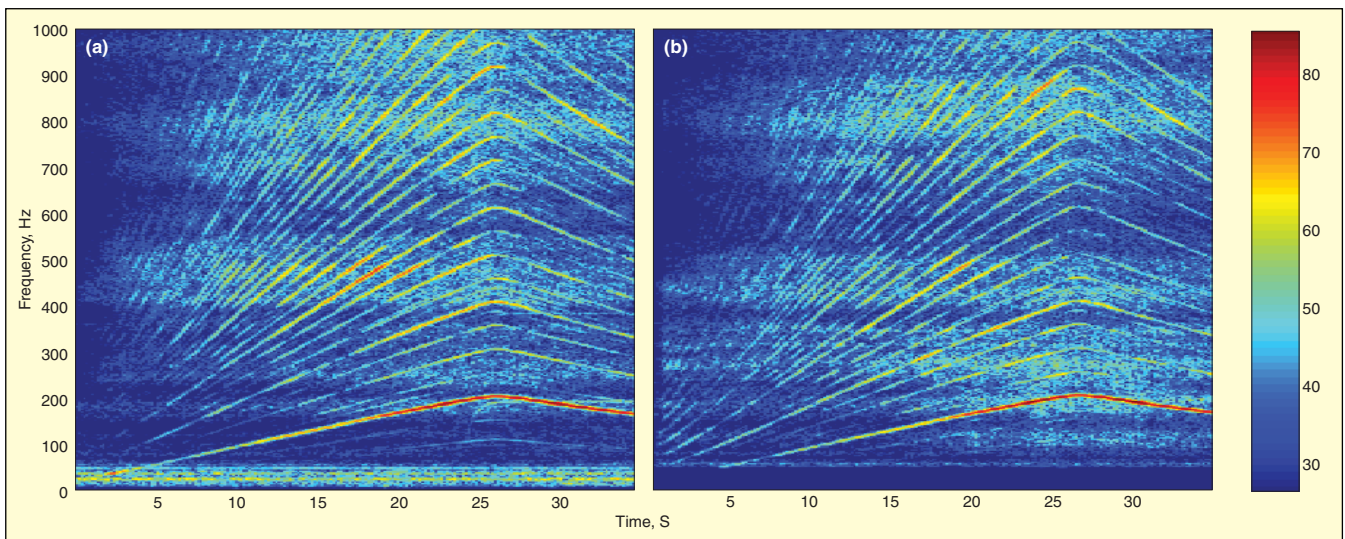


Figure 10. Spectrograms (frequency vs. time) of airborne measured sound (a) and predicted sound (b) at left ear position.

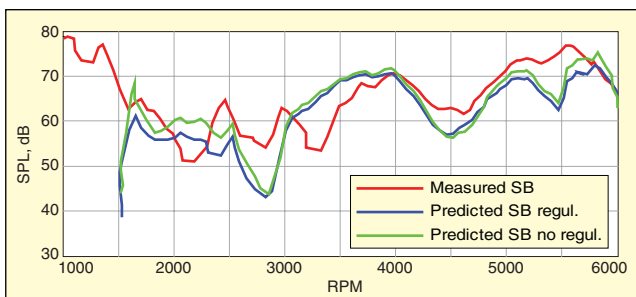


Figure 11. 2nd order contributions – structure-borne measured vs. predicted (with and without regularization applied).

get the second-order contribution prediction given by the green curve. The two curves are not far apart, suggesting that regularization does not have a big effect on the prediction in this frequency range. Overall, there are some deviations between measurement and prediction when comparing structure-borne contributions, but the trends of the curves are the same.

Comparing the airborne prediction with the actual airborne measured sound, we get the spectrograms in Figure 10. The plots are again dominated by the second order, but other orders are also present for this type of excitation. Orders other than the second seem to be predicted very well in this case.

Second-order contributions are again extracted from the spectrograms and plotted together in Figure 12. Very good agreement

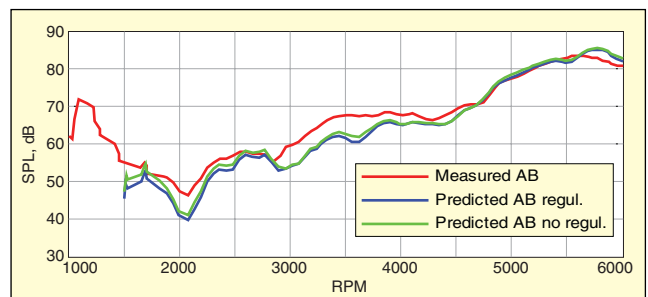


Figure 12. 2nd order contributions – airborne measured vs. predicted (with and without regularization applied).

is observed between measurement and prediction. The effect of regularization for the airborne case at low frequencies has already been noted previously, where we said that since the condition number of the acoustic FRF matrix is so small in that frequency range, the regularization applied will have almost no effect on the predictions. This is evident from the two curves with and without regularization.

Conclusions

Airborne and structure-borne source-path-contribution analysis implemented as a time-domain approach has been shown to produce accurate results for the described set-up using an engine noise and vibration simulator installed in a trimmed vehicle. Inter-


estingly, the method can easily handle standard run-up/run-down engine tests while producing contributions as sounds.

Most of the measurements, which serve as input for the method, were made with the engine installed and making it a practical method. At the same time, we decided to make the models for contribution analysis as simple as possible. For example, the airborne model of engine simulator consisted of only seven point sources, while still making it possible to predict the total airborne noise but also contributions from single engine faces. The simple models with point sources well separated in space will also have an impact on the ill-conditioning of the associated matrices used in the calculating the inverse filters.

The two matrices presented here were only moderately ill-conditioned at higher frequencies, >1 kHz; while at low frequencies, no regularization was needed. This was indicated by the second-order contribution results made for both the airborne and structure-borne cases. However, we believe that the significant ill-conditioning at higher frequencies will have an impact on the actual predicted

sounds produced, changing the balance between low and high frequency content. Further work will go into trying to estimate an optimal threshold, probably frequency dependent, for calculating the inverse filter matrices.

References

1. Verheij, J. W., "Inverse and Reciprocity Methods for Machinery Noise Source Characterization and Sound Path Quantification, Part 1: Sources," *Int. Journal of Acoustics and Vibration*, pp. 11-20, Vol. 2, No.1, 1997.
2. Verheij, J. W., "Inverse and Reciprocity Methods for Machinery Noise Source Characterization and Sound Path Quantification, Part 1: Transmission Paths," *Int. Journal of Acoustics and Vibration*, pp. 103-112, Vol. 2, No.3, 1997.
3. Hansen, P. C., *Rank-Deficient and Discrete Ill-Posed Problems*, SIAM, Philadelphia, PA, 1998.
4. Pedersen, T. F., Herlufsen, H., Hansen, H. K., "Order Tracking in Vibroacoustic Measurements: A Novel Approach Eliminating the Tacho Probe," *Proceedings of SAE*, Traverse City, MI, May 16-19, 2005. 

The author may be contacted at: schuhmache@bksv.com.